

Loader Crane Inertial forces

Domen Rupar

MSc.
University of Ljubljana
Faculty of Mechanical Engineering,
Ljubljana
Slovenia

Jurij Hladnik

MSc.
University of Ljubljana
Faculty of Mechanical Engineering,
Ljubljana
Slovenia

Boris Jerman

Assistant professor, Dr.
University of Ljubljana
Faculty of Mechanical Engineering,
Ljubljana
Slovenia

Slwing cranes are widely used in different areas of transportation. In the paper an example of the loader cranes which are also widely used in timber industry is analysed. These cranes are especially interesting because of their fast movements, the intensive loading spectra and their welded steel arms of lean design, which make them particularly vulnerable regarding the fatigue. A 3D flexible numerical model of the selected Z-type loader crane was created and its movements are simulated on the basis of actual crane operations data. From these simulations the load time histories are determined and furthermore the corresponding load spectrums are extracted using the Rainflow method. It has been shown that due to dynamic effects during acceleration and deceleration of crane movements among the loadings, which must be considered in accordance with the standard fatigue calculation, a number of additional load cycles with smaller amplitudes are introduced into the load histories.

Keywords : loader cranes, spatial movements, numerical simulations, dynamic forces, loading spectrums

1. INTRODUCTION

Loader cranes are extensively used in timber and waste disposal industry. In this paper the Z type loader cranes are discussed which are more and more popular, because of their capability of folding to a relatively small space behind the cab of the lorry transversely to the lorry length, when not being used.

The loader cranes for timber industry are especially interesting for being analysed regarding the inertial loading because of their fast movements of relatively heavy loads, the intensive loading spectra and their welded steel arms of lean design, which make them particularly vulnerable regarding the fatigue cracking.

An important factor in fatigue analyses is estimation of load spectrum applied to the supporting structure under realistic operating conditions. Such estimation can be performed by means of measurements on the existing cranes or by means of simulations.

In the paper [1] by Chang the representative part of the load spectrum was obtained using measurements on real structure during actual operations. The obtained load spectrum was used to determine the remaining service life of the considered crane.

A vital factor of the load spectrum is the dynamic response of the crane's structure due to the swinging of the payload forced by the accelerations and decelerations of the crane. Some of the most recent papers study the dynamic response of the cranes or part of cranes using analytical models.

Posiadala et al. [2] developed the analytical model of the forest crane and simulated the motion of the payload. To get the proper values of dynamic forces and

other dynamical motion parameters the authors take into account also the deformability of the crane's boom.

Sun and Liu [3] have studied the dynamic responses of hydraulic mobile crane during luffing motion. A theoretical model was established using Lagrange's equation and the multi-body theory. Their results show that luffing acceleration has a greater impact on the dynamic response of the crane than the luffing velocity.

Paper [4] (Raftoyiannis and Michaltsos) studies the dynamic behaviour of telescopic crane's boom using the developed analytical model, suitable for dynamic analysis.

The influence of pendulum motion of the payload on the loading of the crane's structure is discussed in [5] by Lee and Kim.

The dynamics of the payload is researched in [6] by Marinović, Sprečić and Jerman. In their study the angles of the payload sway and dynamic forces were attained.

Jerman and Kramar [7] focused their study of the dynamic effect that act on the load suspended of a slewing crane on the horizontal inertial forces.

Some papers study the dynamic response using finite elements models of discussed cranes. Paper [8] by Gašić et al., dealt with a jib crane structure subjected to a moving trolley and payload. Using the FEM they calculated the dynamic responses of the crane's structure. The research takes into account the inertial effects due to the masses of the trolley and the payload.

Ju, Choo and Chui [9] derived a finite elements model of a tower crane in order to study the dynamic response of the crane during luffing motion coupled with the pendulum motion of the payload. They found out that the dynamic response of the crane is dominated with the first few natural frequencies of crane structure and the pendulum motion of the payload.

In this paper a load spectrum of a payload induced force, acting on the tip of the boom of the loader crane is obtained. First, the load carrying structure and the payload are presented together with the assumptions and

Received: September 2015, Accepted: June 2016

Correspondence to: Boris Jerman

University of Ljubljana, Faculty of Mechanical Engineering, Slovenia

E-mail: Boris.Jerman@fs.uni-lj.si

doi:10.5937/fmet1603291R

©Faculty of Mechanical Engineering Belgrade. All rights reserved

FME Transactions (2016) 44, 291-297 291

modelling techniques used. After that the possible crane operations are introduced and the Taguchi method is used for reduction of the investigated combinations. At the end the results are presented and discussed.

2. THE NUMERICAL MODEL OF A CRANE

a. The loader crane L120Z

For the purpose of the research the 3D numerical model of the loader crane L120Z was developed. As the crane load a freshly cut beech wood was selected and different examples of loading and unloading of the vehicle are assumed. For each movement a maximal allowed payload for a given crane position was used. The design service life of the crane is assumed to be 5 years.

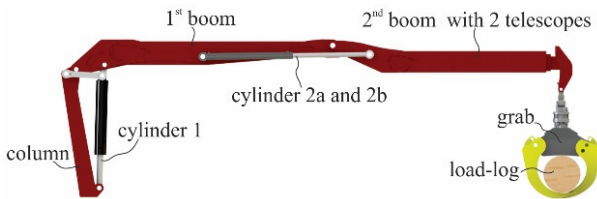


Figure 1: Model of the crane

Figure 1 shows the geometrical crane model with denoted components. The model was created in SolidWorks software according to the drawings, presented on the figures 2, 3, 4 and 5. Figures show the shape and main dimensions of column, 1st boom and 2nd boom with two telescopes.

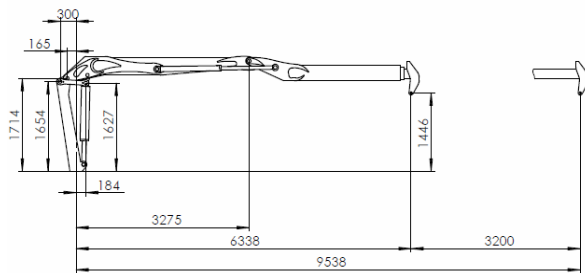


Figure 2: Main dimensions of crane

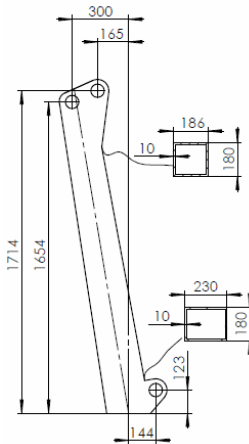


Figure 3: Dimensions and cross section of column

The geometrical model is further imported into Adams View software. The individual parts of the crane are connected to each other using adequate built-in translator and revolute joints.

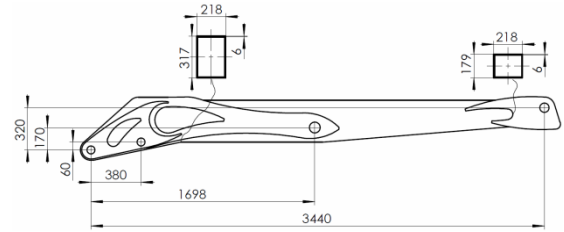


Figure 4: Dimensions and cross section of 1st boom

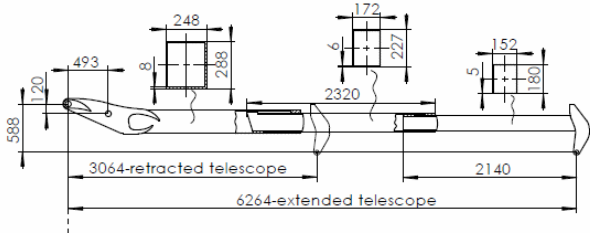


Figure 5: Dimensions and cross sections of 2nd boom and two telescopes

In order to ensure realistic simulations the crane's column, 1st boom and 2nd boom with two telescopes are modelled as flexible bodies using Adams Viewflex. Other elements are assumed to be rigid.

Adams Viewflex uses Modal flexibility to assign eigenvectors to a body; the model designates a system state variable to each eigenvector and calculates the relative amplitude of each eigenvector during a time analysis. The principle of superposition is then used to combine the mode shape to reproduce the total deformation on the flexible body.

In the case of rigid bodies, joints are bound to reference points of the part. When flexible bodies are used we have to connect joints to part of the volume of the body instead. The connection between the joint and the body can be rigid or compliant. In our case the revolute joints were connected to bodies with rigid connections and translating joints between 2nd boom and two telescopes were connected with compliance.

Figure 6 shows the flexible model in Adams View which enables us to determine the loading that is effectively transferred to the crane due to the weight of the log and due to its dynamics in movement.

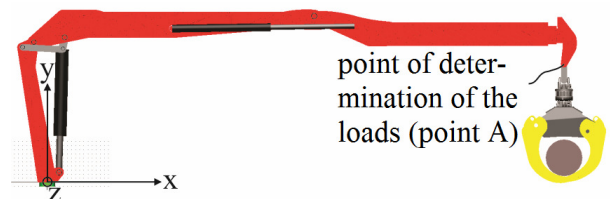


Figure 6: Coordinate system and point of measurement

The corresponding forces were determined at the point where the grab is attached to the 2nd boom (point A in Figure 6). We determined the force components in the x, y and z directions of the Cartesian coordinate system that is placed at the bottom of the column and which rotates with the column (Figure 6).

The position of the crane arm is defined by five variables (shown in Figures 7 and 8):

- rotation of the crane around vertical y-axis by angle δ ,
- rotation of 1st boom around the angle α , measured from horizontal line,

- rotation of the 2nd boom around the z-axis by angle β , measured from horizontal line,
- rotation of the grab around vertical y-axis by angle γ ,
- extension l of the telescopes to achieve the reach R .



Figure 7: Angle γ and δ

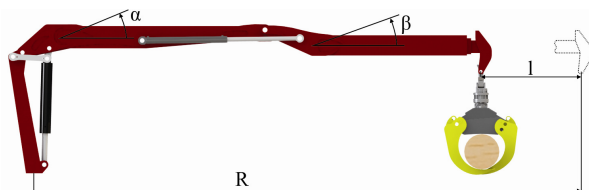


Figure 8: Angles α , β and telescope extension l

b. Crane operations

The movements of the crane were simulated based on the realistic movements of a crane during its lifetime. In this paper we simulated the loading of 5 m logs lengthwise on the trailer. Thus we covered only part of the possible operations of the crane, which are on the other hand covered in more details analysing their varieties.

For description of the varieties of movements of the crane the following influential parameters were considered:

- 1) Initial height of the log;
- 2) Initial reach out of the crane;
- 3) Final height of the crane;
- 4) Rotation of the crane;
- 5) Rotation of the grab;
- 6) The angular velocity of rotation of the crane;
- 7) Moving speed of cylinder 1;
- 8) Moving speed of cylinder 2;

Each parameter was divided into 3 levels.

Parameter 1

The first parameter is the initial height at which the log which must be transported is placed. The height is measured from a plane on which the trailer is positioned. We used the following levels:

- loading from a dell: -3.2 m,
- loading from the ground: 0 m,
- loading from a pile: 3.6 m.

Parameter 2

The second parameter is the initial reach of the crane. Possible initial reach of the crane is conditional upon the initial height of the grab. The following levels were used:

- Minimal possible initial reach at a given height.
- The initial reach defined as an average of the min. and max. initial reach at a given height
- Maximal possible initial reach at a given height

Parameter 3

The third parameter represents the height at which the log is placed on the trailer. These levels were used:

- empty trailer: 1.5 m,
- half loaded trailer: 2.6 m,
- completely loaded trailer: 3.6 m.

Parameter 4

In the fourth parameter is the rotation of the crane. We wanted to include typical working range of the crane, therefore the following levels were set:

- rotation for $\delta=50^\circ$,
- rotation for $\delta=90^\circ$,
- rotation for $\delta=130^\circ$.

Parameter 5

When loading the crane, in some cases there is a need for rotation of the log. Hence the fifth used parameter is the rotation of the grab. The following levels of the parameter were used:

- rotation for $\gamma=0^\circ$,
- rotation for $\gamma=45^\circ$,
- rotation for $\gamma=90^\circ$.

Parameter 6

On the basis of video analysis it was established that the crane needs approximately 6 s to rotate for 90° . Based on this assessment we estimated the angular velocity of the crane. This value represents one level of the sixth parameter. For the remaining levels we reduced and increased the time of rotation of the crane for 90° by 1 s. The levels were therefore set as follows:

- rotation for 90° in 5 s,
- rotation for 90° in 6 s,
- rotation for 90° in 7 s,

Parameter 7

On the basis of analysis of video footage of the real crane's operations, it was estimated that the 1st boom luffs for an angle of 45° in about 6 s. Based on this assessment we estimated the luffing angular velocity of the 1st boom which represents one level of the parameter. For the remaining levels we reduced and increased the luffing time for 45° by 1 s. We therefore used the following levels:

- luffing for 45° in 5 s,
- luffing for 45° in 6 s,
- luffing for 45° in 7 s.

Parameter 8

From video footage of the loading of the trailer, it was estimated that the 2nd boom luffs for an angle of 50° in about 5 s. Based on this assessment we estimated the angular velocity of the luffing of the 2nd boom, which represents one level of the parameter. For the remaining levels we reduced and increased the time of luffing for 45° by 1 s:

- luffing for 45° in 4 s,
- luffing for 45° in 5 s,
- luffing for 45° in 6 s.

c. Selection of representative combinations

It would be necessary to perform $3^8 = 6561$ analysis if all possible crane movements should be analysed, based on the combinations of the proposed values of the selected parameters.

With the aim of reduction of the required number of parameter combinations which must be analysed the Taguchi method [10] which reduces the number of combinations without losing the statistical significance of individual parameters is employed.

The Taguchi method uses orthogonal fields - a set of combinations of parameters on different levels - for planning of the experiment. The size of the orthogonal field depends on the number of parameters chosen and number of levels of the individual parameter. In observed case of 8 parameters on 3 levels an orthogonal field L18 is used. For the implementation of the Taguchi method, each operation of the crane was divided into six sections:

1. Section: Raising the 1st boom by employing cylinder 1;
2. Section: The contraction of the telescope;
3. Section: The contraction of the crane by employing cylinders 1 and 2;
4. Section: Rotation of the crane and grab;
5. Section: Movements of the 1st boom by employing cylinder 1
6. Section: Lowering of the 2nd boom by employing the cylinder 2

Table 1 shows values of angles α , β for each individual level of the influential parameters 1, 2 and 3. It also shows the extension of the telescopic boom of the crane at each height because of the values of angles depend on it.

Table 1: Values of α , β and l

	Height [m]	R[m]	α [°]	δ [°]	l[m]
Initial position	-3.2	3.77	0	-80	2.56
		4.56	0	-71	2.59
		5.35	5	-65	3.2
	0	3.93	10	65	0
		6.67	20	-37	2.05
		8.92	5	-20	3.2
	3.6	3.24	70	-25	0
		6.25	50	-9	1.54
		8.72	35	-1	3.2
Final position	1.5	3.08	40	-65	0
	2.6	3.03	65	-45	0
	3.6	3.24	70	-25	0

The rotation of the crane was carried out for all the selected crane movements in the following position:

- $\alpha=55^\circ$,
- $\beta=0^\circ$,
- $l=0$ m.

Table 2 shows the example of changing of five variables that define the individual positions of the crane during crane movement, defined by combination 1.

Table 2: Movement combination 1

Combination	α [°]	β [°]	δ [°]	l [m]	γ [°]
1	0	-80	0	1.28	0
	30	-50	0	1.28	0
	30	-50	0	0	00
	55	0	0	0	0
	55	0	50	0	0
	40	-15	50	0	0
	40	-65	50	0	0

Every rotation is carried out in three stages. In the first stage a uniformly accelerated motion is used to achieve the required angular velocity (Fig. 9, time t_1). In the second stage the uniform rotation is employed (Fig. 9, time t_2). In third stage (Fig. 9, time t_3) a uniformly decelerated is used to slow down the rotation to the stand still, when the angular velocity obtain the value of 0 (Fig. 9, time t_4).

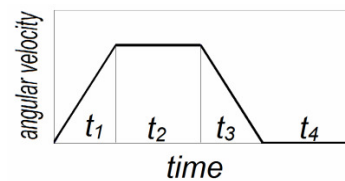


Figure 9: Three stages during the rotation

The acceleration and deceleration time of each rotation is based on observation of realistic movements. These times are set as follows:

- column: 0.5 s,
- 1st boom: 0.55 s,
- 2nd boom: 0.55 s.

Based on the required rotation angle, duration of rotation and the acceleration and deceleration times the angular accelerations of the column, 1st and 2nd boom are determined. The maximal angular velocities, which must be achieved, are also calculated.

In every considered operation the lifting and lowering of the log is also included. During lifting the weight of the log is not transferred to the crane suddenly but gradually, as the force in the connection between the grab and the top of the boom rises gradually. Because of in the developed model the log is permanently fixed on the grab, the lifting of the log was modelled using an additional force which acts on the log. The force is of the same size, but of opposite direction as the force of gravity of the log and was gradually reduced to 0 in 0.5 s, simulating gradual loading of the crane. The same procedure, but in the opposite direction, is carried out at the end of the movement when the gradual disposal of the log to the trailer is simulated. At that occasion the force is increased from 0 to the weight of the log in 1s.

d. The crane payload

A typical load of a loader crane is a log of a length of 5 m. In this paper a log is modelled using a 5 m long cylinder. The anticipated material of the log is freshly cut beech wood with the density of around 1200 kg/m^3 . Such diameter of the cylinder was adapted for the individual simulated case to ensure the weight of the cylinder equal to the load capacity of the crane at its maximum extension in that particular case.

Table 3 shows the diameter and masses of logs for all selected cases.

Table 3: Log diameter and mass

Combinations	Diameter of log [mm]	Mass of log [kg]
1-6	600	1700
7-9	510	1230
10-12	636	1910
13-15	553	1440
16-18	474	1060

e. Implementation of movements

For the implementation of motions of selected crane operations the inverse kinematics is used. In first step the necessary changes of angles α , β and δ for each operation are established. Then a program in Excel is written to determine the course of changing of angles for individual movement and to calculate the necessary movements of the hydraulic cylinder. These movements were assigned to appropriate cylinder in the model.

From the simulations successfully carried out the results in the form of the load time histories at point A were obtained for all three force components. Then, using the Rainflow counting algorithm, the load cycles for each direction were counted and arranged into classes. In such a way the load spectrums of the components of the crane loading force were determined for the selected 18 representative cases. These load spectrums must be further extrapolated to cover the complete service life of the crane.

3. RESULTS

a. Simulation results

The results of the simulations can be revealed in graphs. As an example the representative cases 1, 9 and 18 are shown in Figs. 10 to 15.

In Fig. 10 the vertical force F_y for the case number 1 is introduced. It can be seen the increase of the force during the load lifting period, its oscillations during the load transportation and its decreasing during the load discard. The remaining force represents the weight of the grab.

From the curve of the angle δ in the Fig. 11, the times of start of the rotation and of end of the rotation of the crane can be read out. From Fig. 10 can be further analysed how the tangential force F_y is related with this movement.

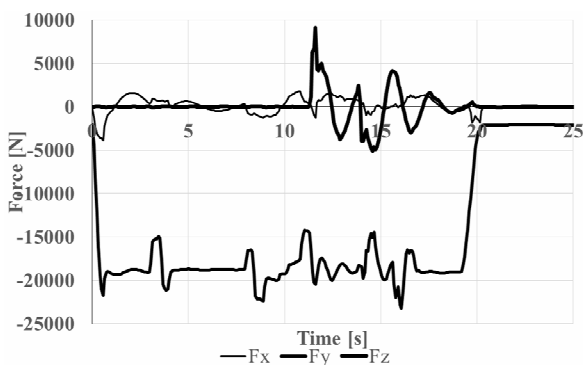


Figure 10: Forces in radial, vertical and tangential direction for the representative case 1

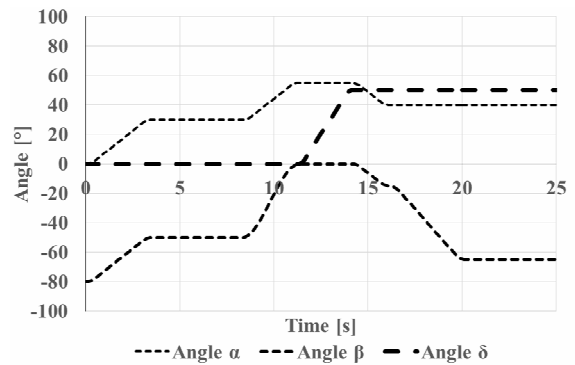


Figure 11: Angles α , β and δ for the representative case 1

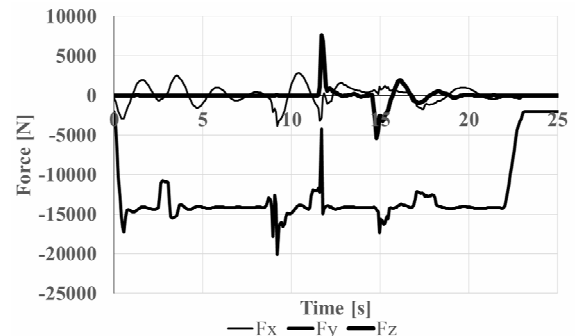


Figure 12: Forces in radial, vertical and tangential direction for the representative case 9

In Fig. 11 the luffing angles of the crane first arm α and of the crane second (telescopic) arm β are also shown. It can be seen that in the initial crane position the first arm is in the horizontal position and the second arm is almost in the vertical position. By lifting the first arm, the second arm also rotates, while the relative angle between them stays constant till around 8 seconds. After that the second arms luffing is faster. At around 14 seconds, both angles start to decrease until they reach their end position.

Similar observations can be done also for the Figs. 12 -15, where results for cases number 9 and 18 are shown.

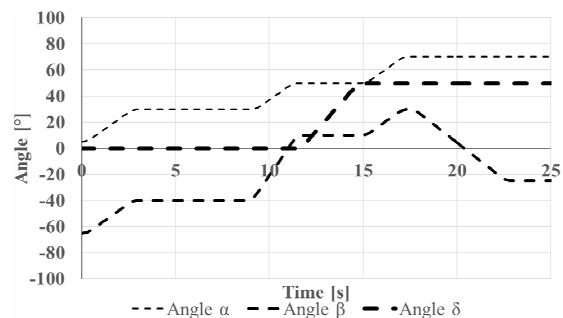


Figure 13: Angles α , β and δ for the representative case 9

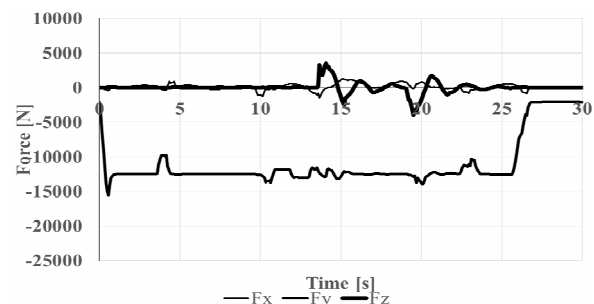


Figure 14: Forces in radial, vertical and tangential direction for the representative case 18

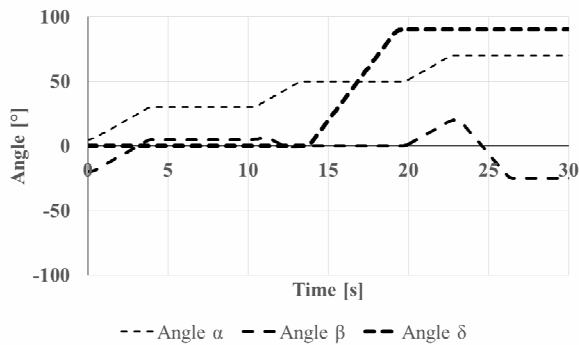


Figure 15: Angles α , β and δ for the representative case 18

b. Extrapolation of results

The extrapolation of simulation results is carried out in a simplified way. The results are multiplied by the ratio between the number of operating cycles in service life and the number of simulated operating cycles.

To calculate the total number of operating cycles of the crane in its service life the following data is used:

- service time: 5 years,
- number of operating days per year: 250 days,
- number of effective working hours per day: 2 h,
- number of operating cycles performed in one minute: 2 cycles/minute.

The total number of operating cycles is assumed to be 300000, therefore the results, gained with the simulations must be multiplied by a factor of 16667 to be extrapolated to the entire service life of the crane.

c. Load spectrums

The load spectrum of the force in the x direction is shown in graph in 16. The force F_x is the result of the centrifugal force due to the rotation of the crane and the load oscillations around z axis. The total number of load cycles in x direction is 4183417. The smallest load of 0.612 kN is present in 2133376 cycles. On the other hand the largest load of 8.588 kN is present in only 16667 cycles.

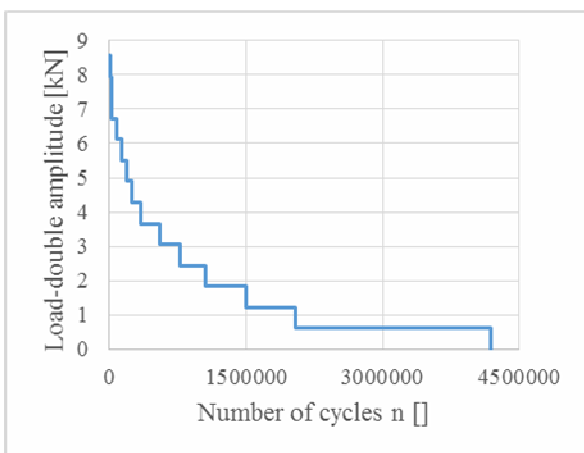


Figure 16: Load spectrum of the force component F_x (radial direction)

It can be seen from the load spectrum that there are many load cycles with small double amplitude (force range), and a small number of cycles with a large

double amplitude. Small double amplitudes are primarily result of oscillations of the log whereas larger double amplitudes are connected with the centrifugal force due to the rotation of the crane.

Figure 9 shows the load spectrum for the force in the y direction. The force F_y mainly depends on the weight of the log. The minimum load in y direction occurs in 1983376 cycles and equals 1.528 kN. The maximum load, which is caused by the maximal weight of the load, is 21.392 kN and the number of cycles with this load is 66668. The total number of load cycles in y direction is 3383401.

From Figure 9 we can clearly see two different parts of the spectrum. The first part presents cycles with large double amplitude. These large force ranges are present in a small number of cycles. Cycles in this part are directly related to the weight of the load. The second part of the graph consists of a number of cycles with small double amplitude. The cycles are associated with the dynamic forces caused by the oscillations of the log on the crane steel structure.

Figure 10 displays the load spectrum for the force in the z direction. Force F_z is induced due to the rotation of the crane and oscillations of the log around x axis. The total number of load cycles is 1816703. The smallest load is 1.12 kN and is present in 800016 cycles. 33334 cycles have the largest double amplitude of 15.688kN.

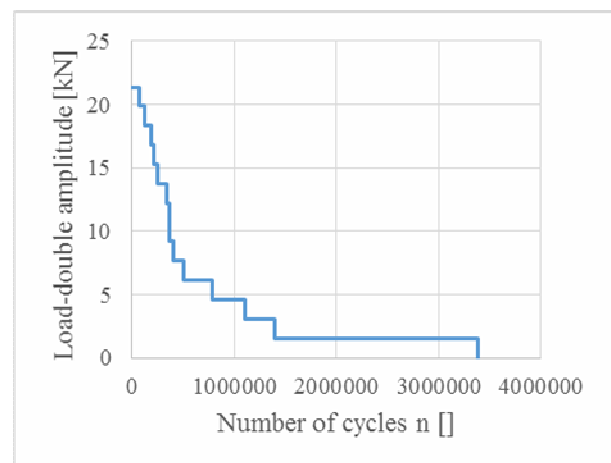


Figure 9: Load spectrum of the force component F_y (vertical direction)

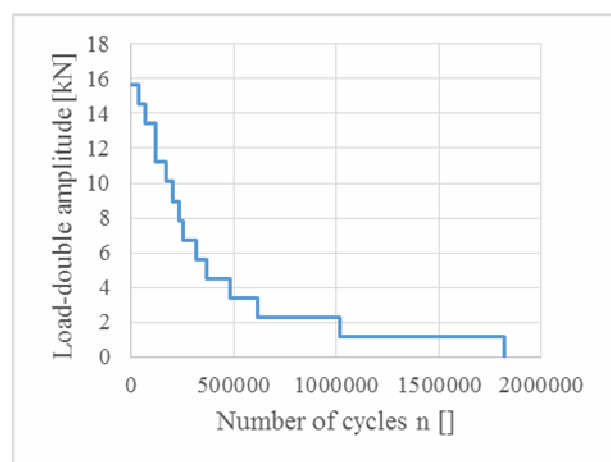


Figure 10: Load spectrum of the force component F_z (tangential direction)

Examination of result in Figure 10 shows similar characteristics as are shown in Figures 16 and 17. A large number of cycles with small double amplitude are present in spectrum. These cycles are result of the oscillations of the load around the x axis. If we look at the beginning of the spectrum we notice a small number of loads with large double amplitude. These cycles are the result of the accelerations and decelerations of rotation of the crane and the associated dynamic behaviour of the log.

4. Conclusion

A study of the dynamic forces acting on the load carrying structure of the loader crane during its operation was performed. Simulations were carried out using the developed 3D numerical model of the crane. The number of investigated combinations was reduced using the Taguchi's method from 6561 to 18, without losing the legitimacy of the results. From calculated load-time histories of components of the force acting on the crane in point A, the corresponding load spectrums were determined using the Rainflow method.

It was discovered that a large number of cycles with a small double amplitude are present for force components in all three directions (F_x , F_y and F_z). These cycles are in mostly a result of pendulum motion of the payload.

ACKNOWLEDGEMENT

Authors would like to express a special thanks to the Tajfun Planina d.o.o. and the Tajfun Liv d.o.o. who enabled and supported the research.

REFERENCES

- [1] Chang Y.: Fatigue Life Evaluation of a Grab Ship Unloader, China Steel Technical Report, No. 23, 2010, str. 36-41
- [2] Posiadala B., Warys P.; Cekus D.; Tomala M.: The Dynamics of the forest crane during the load carrying; International Journal of Structural Stability and Dynamics, Vol.13, No.7,2013
- [3] Sun G.; Liu J.: Dynamic responses of hydraulic crane during luffing motion; Mechanism and machine theory; Vol. 41, No. 11, pp. 1273-1288, 2006
- [4] Raftoyiannis I.G.; Michaltsos G.T.: Dynamic behaviour of telescopic cranes boom; International Journal of Structural Stability and Dynamics, Vol.13, No.1, 2013

- [5] Lee, J.-W., Kim, D.-H.: Dynamics of a spreader suspended by four flexible cables. Proceedings of the Institution of Mechanical Engineers, Part C, Journal of Mechanical Engineering Science, 2004, 218(10), 1125-1138
- [6] Marinović I.; Sprečić D.; Jerman B. A Slewing Crane Payload Dynamics. // Tehnički vjesnik-Technical Gazette, Vol. 19, No.4, pp. 907-916, 2012
- [7] Jerman B.; Kramar J.: A study of the horizontal inertial forces acting on the suspended load of slewing cranes, International journal of mechanical sciences, Vol. 50, No. 3, pp. 490-500, 2008
- [8] Gašić V.; Zrnić N.; Rakin M.; Consideration of a moving mass effect on dynamic behaviour of a jib crane structure; Tehnički vjesnik-Technical Gazette, Vol. 19, No. 1, pp.115, 2012
- [9] Ju F.; Choo Y.S.; Cui F.S.: Dynamic response of tower crane induced by the pendulum motion of the payload; International journal of solids and structures, Vol. 43, No. 2, pp. 376-389, 2006
- [10] Taguchi, G.: System of Experimental Design, Dearborn, Michigan, American Supplier Institute, 1987

СИЛЕ ИНЕРЦИЈЕ КОД ДИЗАЛИЦА УТОВАРИВАЧА

Д. Рупар, Ј. Хладник, Б. Јерман

Обртне дизалице имају широку примену у различитим областима транспорта. Анализира се један пример дизалице утоваривача која се користи у дрвној индустрији. Овакве дизалице су интересантне за анализу због великих брзина кретања, интензивних спектра оптерећења и витких заварених челичних стрела, што их чини посебно осетљивим на замор. Израђен је 3Д нумерички модел дизалице утоваривача Z типа. Симулација кретања је извршена на основу података кретања реалне дизалице утоваривача. Симулацијама је одређена временска историја оптерећења, док су одговарајући спектри оптерећења одређени помоћу методе бројања кишних капи (Rainflow). Показано је да се, осим оптерећења која се морају узети у обзир сагласно стандардним прорачуном замора, услед динамичких утицаја у периодима убрзања и успорења дизалице појавио и одређени број додатних циклуса оптерећења са мањим амплитудама.